How to cite: *Angew. Chem. Int. Ed.* **2020**, *59*, 22779–22784
International Edition: doi.org/10.1002/anie.202009303
German Edition: doi.org/10.1002/ange.202009303

Ligand Design

α-Cationic Phospholes: Synthesis and Applications as Ancillary Ligands

*Tim Johannsen, Christopher Golz, and Manuel Alcarazo**

Abstract: *A series of structurally differentiated α-cationic phospholes containing cyclopropenium, imidazolium, and iminium substituents has been synthesized by reaction of chlorophosphole* ***1*** *with the corresponding stable carbenes. Evaluation of the donor properties of these compounds reveals that their strong π-acceptor character is heavily influenced by the nature of the cationic group. The coordination chemistry of these newly prepared ligands towards* Au^{I} *centers is also described and their unique electronic properties exploited in catalysis. Interestingly, α-cationic phosphole containing catalysts were not only able to accelerate model cycloisomerization reactions, but also to efficiently discriminate between concurrent reaction pathways, avoiding the formation of undesired product mixtures.*

Introduction

In sharp contrast to pyrrole, which is a planar and strongly aromatic heterocycle, its immediately heavier analogue, phosphole, is characterized by a highly pyramidalised arrangement of the substituents around the phosphorus and, as consequence, a severely diminished degree of aromaticity.[1] This geometry is adopted due to the high energetic cost required to planarize the phosphorus atom, which is not compensated by the aromatic stabilization won in a hypothetically planar conformation, even though theoretical calculations predict that in such planar environment phosphole would be more aromatic than pyrrole.[2] Hence, in phospholes the P-lone pair is bent away from the heterocycle and its overlap with the butadienyl fragment is drastically reduced.[3] This fact primarily defines the different reactivities of phospholes and pyrroles; in particular, the possibility of the former to form P-oxides, quaternary salts, or metal complexes by reaction at phosphorus.[4]

With regard to the use of phospholes as ancillary ligands, both experimental and theoretical analyses indicate that while they depict very similar σ-electron-releasing properties to these characteristic of classical phosphines of analogue structure; their low lying LUMO, which largely corresponds to the mixture of the exocyclic σ*(P-R) with a π*-orbital, confers them stronger π-acceptor character.[5] This results in enhanced back-donation from orbitals of the metal and, subsequently, in lower net electronic transfer to the metal centres they coordinate (Figure 1).[6]

During the last few years, our group has established a research program focused on the design and synthesis of strong acceptor ancillary ligands. These have been utilized to promote transformations in which the energetic span (δE) of the complete catalytic cycle is minimized by the enhancement of the electrophilicity of the metal.[7] Specifically, we have prepared a complete series of α-cationic ligands by formal exchange of at least one -R substituent on typical phosphines by positively charged groups, such as cyclopropenium, imidazolium or pyridinium rests. Using this design, a series of Au^{I}, Pt^{II} and Rh^{I} catalysts depicting unmatched reactivity in hydroarylation[8] and cycloisomerization reactions[9] have been developed, together with enantioselective versions of the already mentioned processes.[10]

Given the intrinsic π-acceptor character that the phosphole architecture imposes to ligands derived from that heterocycle, we envisaged that such platform might be an ideal starting point to develop even stronger π-acceptor ligands by incorporation of positively charged substituents as exocyclic rests. In the resulting α-cationic phospholes the electron withdrawing effect of the cationic group should lead to a larger localization at phosphorus of the σ*(P-R) orbital, favouring the σ*(P-R)-π*(ring) mixture and, as consequence, lowering the energy of the LUMO (Figure 1). Modulation of this interaction by employing cationic groups of different nature should additionally allow the fine tuning of the π-accepting properties of the final α-cationic phosphole.

[*] T. Johannsen, Dr. C. Golz, Prof. Dr. M. Alcarazo
Institut für Organische und Biomolekulare Chemie, Georg-August-Universität Göttingen
Tammanstr. 2 Göttingen (Germany)
E-mail: malcara@gwdg.de
Supporting information and the ORCID identification number(s) for the author(s) of this article can be found under: https://doi.org/10.1002/anie.202009303.

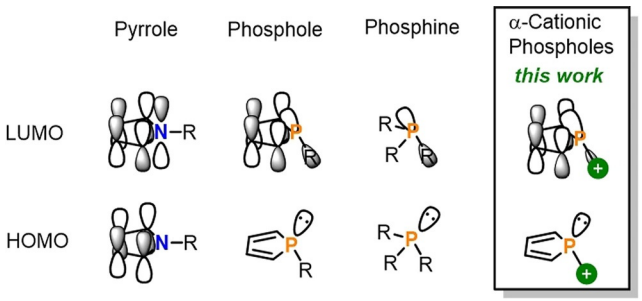

Figure 1. Frontier orbitals in phospholes and impact of the cationic rest on the LUMO energy.

Herein, the synthesis of such cationic phospholes is reported for the first time, their structure elucidated by means of NMR spectroscopy and X-ray crystallography, and their donor properties evaluated. Finally, their coordination chemistry towards Au^{I} centres is studied, and the first practical applications in homogeneous catalysis of the obtained complexes are described.

Results and Discussion

Synthesis and Structure of α-Cationic Phospholes

The preparation of a prototype imidazolium-substituted phosphole was initially envisaged by reaction of 4,5-di-(Me)IMes with tetraethyl-substituted chlorophosphole **1**, which was synthesized using the available routes.[11] After anion exchange with $NaSbF_6$ and washing of the crude reaction mixture with *n*-pentane, **2a** was isolated as a white solid in 76% yield. In an analogue manner adducts **2b**, **2c** and **2d** where obtained by reaction of **1** with 1,2-(diisopropylamino) cyclopropenyl-1-ylidene[12] or cAACs of different steric demand,[13] respectively (Scheme 1). The $^{31}P\{^{1}H\}$NMR of these adducts display characteristic resonance signals at $\delta =$ −38.3 (**2a**), −41.0 (**2b**), −16.0 (**2c**) and 0.8 ppm (**2d**). Compared with that of 1-phenyl-2,3,4,5-(tetraethyl)phosphole ($\delta = 3.0$ ppm), the significant up field shift of **2a**, **2b** and **2c** can be attributed to the effect of the positively charged groups (Scheme 1).[7b,c] The shift of the ^{31}P signal in **2d** cannot be compared due to the tremendous steric hindrance of the Ad(cAAC) fragment, which significantly alters the geometry of the ligand.

The connectivity of salts **2a–d** was subsequently confirmed by X-ray crystal analysis (See Figure 2 for the ORTEP plots, and the Supporting Information). In these structures the C1-P1 distances do not significantly differentiate along the series (1.80–1.86 Å), which are in the range of typical values for P−C(sp^2) bonds.[14] In addition, the sum of angles around P1: 302.64(12)°, **2a**; 304.47(18)°, **2b**; 295.00(52)°, **2c**; and 311.11(18)° for **2d**, indicate that the central P atom adopts a pyramidal environment; albeit the pyramidalization slightly diminishes when bulkier cationic substituents need to be accommodated. Finally, in the solid state the P-atoms of **2a–d**, are displaced out of the plane defined by the butadiene moiety (0.46 Å in **2a**; 0.39 Å in **2b**; 0.47 Å in **2c**; and 0.78 Å in **2d**). These parameters, together with the alternation of the C−C bond distances in the butadiene moieties corroborate the lack of aromatic character in the phosphole ring, something already known for the non-charged members of the family as well (see the Supporting Information).

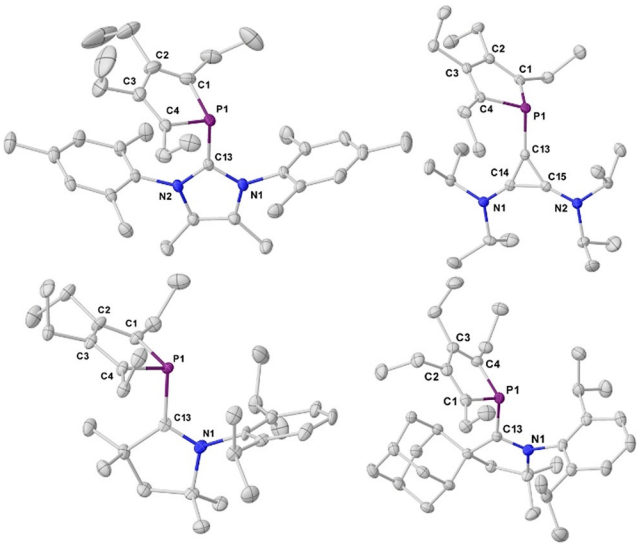

Figure 2. X-ray structures of **2a–d**. Hydrogen atoms, SbF_6 counterions and solvent molecules are removed for clarity; ellipsoids are set at 50% probability.[15].

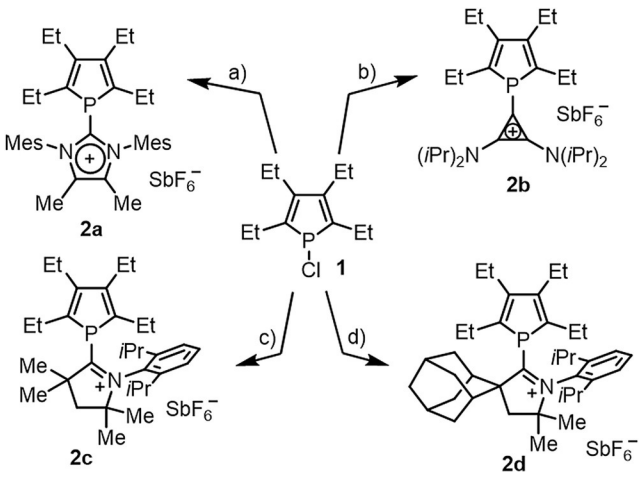

Scheme 1. Synthesis of α-cationic phospholes. Reagents and conditions: a) 1,3-dimesityl-4,5-dimethylimidazol-1-ylidene (1.0 equiv), Et_2O, −78 °C, 2 h, and then $NaSbF_6$, −78 °C→r.t., 76%; b) 2,3-diisopropylaminocyclopropenyl-1-ylidene (1.0 equiv), otherwise as a), 76%; c) Di-(Me)cAAC (1.0 equiv), otherwise as a), 60%; d) AdcAAC (1.0 equiv), otherwise as a), 46%.

Stereoelectronic Properties of α-Cationic Phospholes

IR stretching frequencies in *trans*-[RhCl(CO)L_2] complexes are generally used to evaluate the donor endowment of new ligands and establish their Tolman electronic parameter (TEP). Hence, we initially prepared complex **3b** by reaction of $[RhCl(CO)_2]_2$ with **2b**. Comparison of the IR spectrum of **3b** ($\upsilon_{CO} = 1984\ cm^{-1}$) with that of **4** ($\upsilon_{CO} = 1971\ cm^{-1}$), which contains a phosphine bearing a cyclopropenium substituent as well but no phosphole unit reveals, within experimental error, that **2b** is a weaker net donor ligand.[16] This is attributed to the stronger acceptor properties imparted by the phosphole architecture (Scheme 2). Probably due to their excessive steric demand, ligands **2a** and **2c**,**d** do not form *trans*-[RhCl(CO)L_2] complexes by reaction with $[RhCl(CO)_2]_2$ making this method inappropriate to compare their donor properties.[17] The X-ray structure of **3b** has been resolved and is shown in the Supplementary Information.

Hence, the oxidation potential $E_p(ox)$ was chosen as an alternative parameter to rank the electronic properties of the

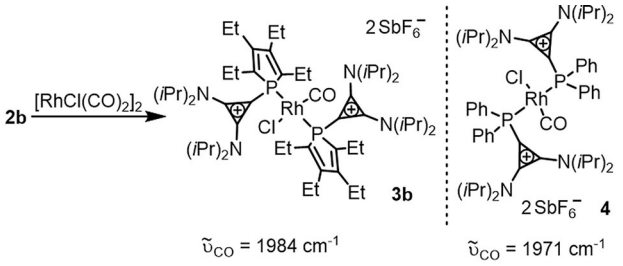

Scheme 2. Synthesis of **3b** and comparison of its υ_{CO} with that of **4**.

new ligands. Cyclic voltammetry measurements afford the following values for the oxidation of ligands ($E_p(ox) = 1.32$ V, **2a**; 1.18 V, **2b** and 1.46 V, **2c**, calibrated versus Fc^+/Fc), which suggest that **2a** and **2b** are, respectively, slightly better and worse donors than $(MeO)_3P$ (1.287 V). Ligand **2c**, due to the acceptor properties of the cAAC moiety, stands as the less basic member of the series. Its $E_p(ox)$ is very similar to the ones measured for α-dicationic phosphines.[7a] These values however, should be considered with caution because of the irreversible nature of the oxidations monitored. The percent buried volume ($\%V_{Bur}$) and the topographic steric maps of **2a–d** are shown in Figure 3. Given the quite rigid nature of the core architecture of these ligands (in particular **2a**, **2c**,**d**), which strongly limits the impact of conformational changes in solution; it can be concluded that upon coordination **2a** and **2c**,**d** impose a geometry around the metal center very similar to that created by Buchwald biaryl phosphines, while this privileged environment cannot be provided by the more flexible **2b**.[18]

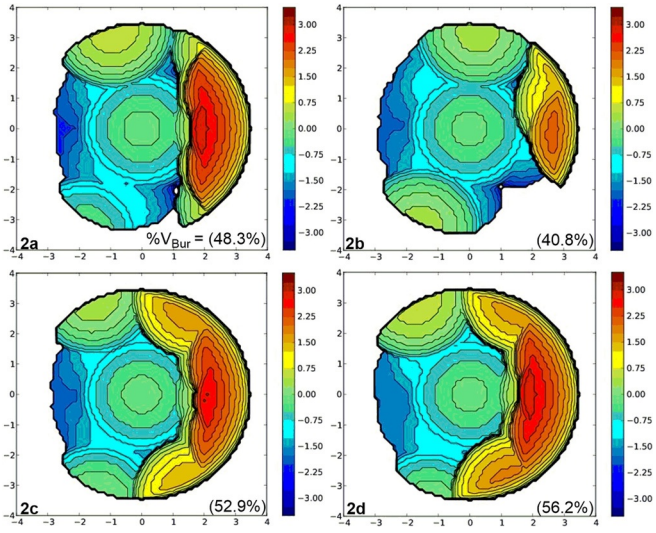

Figure 3. Topographic steric maps for **2a–d**.

Synthesis of α-Radical Phospholes

Notably, during the electrochemical analyses, reversible reduction peaks were observed at −1.512 V and −1.306 (vs. Fc/Fc^+) for **2c**, and **2d**, respectively, which provided evidence of the stability of the corresponding neutral α-radical phospholes. Encouraged by this result, we embarked on the isolation of these species. By treatment of the cationic precursor **2c** with one equivalent of potassium in graphite (KC_8) in tetrahydrofuran (THF) at −78 °C, a deep-green solution was obtained, from which radical **5c** was isolated as black solid in moderate but reproducible yield (Figure 4a). Crystals suitable for X-ray analyses of this compound were grown by cooling their respective saturated pentane solutions to −20 °C. The C1-P1 distance in **5c** (1.7976(9) Å) is notably shorter than that in their cationic precursor **2c** (1.867(6) Å), while the elongation of the C1–N1 bond in radical **5c** (1.309(8) Å in **2c** and 1.3960(11) Å in **5c**) is consistent with a lesser degree of π-bonding between these two atoms as expected from a of the partial population of the C-N π*-orbital (Figures 4b and 5).

A deeper insight into the electronic structure of **5c** was gained by X-band electron paramagnetic resonance (EPR) measurements from samples dissolved in dry toluene. The isotropic spectrum (Figure 4c) shows a g factor of 2.0028, which is consistent with an essentially C-based radical. Additionally, the resolved hyperfine splitting of the spectra

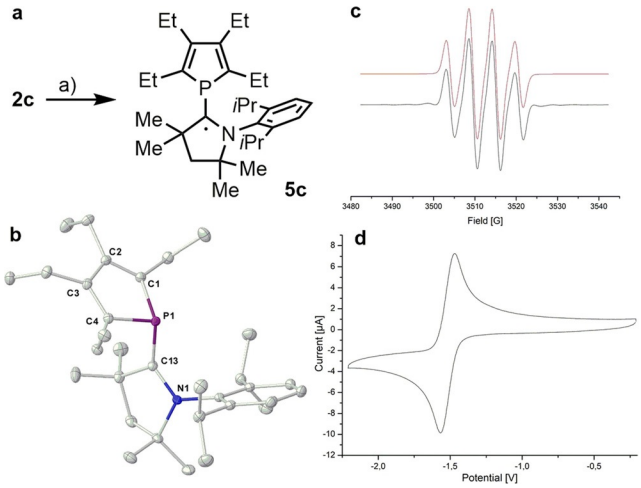

Figure 4. a) Synthesis of **5c**. Reaction conditions: KC_8, THF, −78 °C, 30%; b) X-ray structure of **5c**, hydrogen atoms were removed for clarity and ellipsoids are set at 50% probability.[15] c) Experimental (black) and simulated (red) X-band EPR spectra of **5c** ($g = 2.0028$, $a_P = 5.36$ G, $a_N = 5.62$ G) in toluene solution at r.t. (G = gauss); d) Cyclic Voltamogram of **5c** in CH_2Cl_2 calibrated versus $Cp^*_2Fe/Cp^*_2Fe^+$, Bu_4NPF_6 (0.1 M).

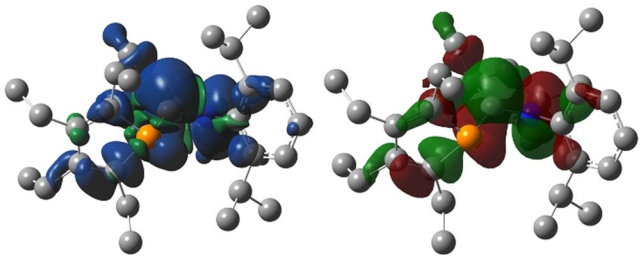

Figure 5. a) Calculated spin densities of **5c** (left) and b) SOMO plot (right) at the UB3LYP-D3/def2-TZVP level. Total spin density drawn at an isosurface value of 0.0005 and SOMO drawn at 0.025.

reveals delocalization of spin density onto the adjacent N1 and P1 atoms; the quartet spectrum observed for **5c** is the result of hyperfine coupling constants that are apparently identical ($a_P = 5.36$ G; $a_N = 5.62$ G).[19]

DFT calculations were performed at the UB3LYP-D3/def2-TZVP//UTPSS/def2-TZVP level[20] (see the Supporting Information for computational details). These calculations accurately reproduce the geometries observed experimentally in the solid state for **5c** and provide a quantitative picture of the spin distribution (Figure 5). As can be seen from the plots of the localized Mulliken spin densities and that of the singly occupied molecular orbital (SOMO), the unpaired electron density is mainly located at the original carbene carbon atom derived from the cAAC fragment (ca. 68%). Moreover, there is considerable spin density on the N atom (ca. 21%), and only some residual one at the P center (less than 1%).

Synthesis of Au^I Complexes

Encouraged by this analysis and willing to exploit the stereoelectronic properties of the newly prepared α-cationic phospholes in catalysis, the corresponding Au^I derivatives **6a–d** were prepared by reaction of $(Me_2S)AuCl$ with phospholes **2a–d**, respectively (Scheme 3). Very indicative of the formation of the desired Au^I-complexes is the downfield displacement of the $^{31}P\{^1H\}$NMR chemical shifts upon coordination; $\delta = -2.1$ (**6a**); −2.2 (**6b**); 15.4 (**6c**); and 26.3 ppm (**6d**). The decision to employ Au-catalysis for the initial screening of α-cationic phospholes as ancillary ligands comes from our experience in Au-catalyzed processes, which often benefit from strong acceptor ligands, and other literature precedents.[21]

The solid-state structures of complexes **6a–d** were determined by X-ray diffraction analysis. The ORTEP diagrams of **6b** and **6c** are shown in Figure 6, and those of **6a** and **6d** can be found in the Supporting Information. The measured Au1-P1 bond lengths for these complexes, 2.2238(9) Å, **6a**; 2.233(3) Å, **6b**; 2.2151(6) Å, **6c** and 2.2283(9) Å, **6d**; are

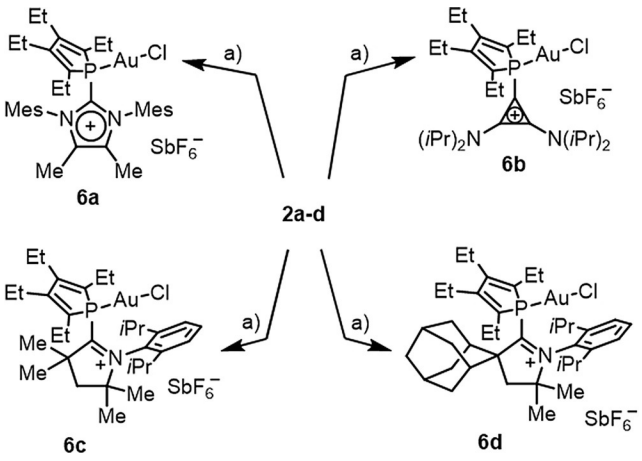

Scheme 3. Synthesis of Au^I complexes **6a–d**. Reagents and conditions: a) $(Me_2S)AuCl$ (1.0 equiv), CH_2Cl_2, rt, 3 h, **6a** (95%); **6b** (78%); **6c** (82%); **6d** (78%).

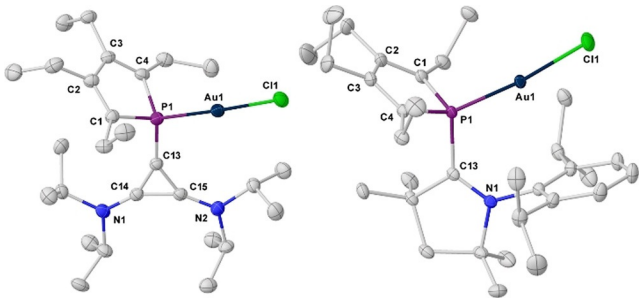

Figure 6. X-ray structures **6b** and **6c**. Hydrogen atoms and counter-anions were removed for clarity; ellipsoids are set at 50% probability.[15]

identical to the ones measured for neutral phosphole-Au^I complexes (P1-Au1, 2.20–2.24 Å).[17,22] Moreover, in structures **6a**, **6c**,**d**, a short contact between the Au atom and the C_{ipso} from the flanking aryl ring (3.0949(35) Å, **6a**; 3.1691(22) Å, **6c**; 2.9757(32) Å, **6d**) can be observed.[23] In all cases the geometry of the P-Au-Cl fragment is slightly distorted from the expected linearity (P1-Au1-Cl1 angles: 176.5° in **6a**; 175.1° in **6b**; 173.2° in **6c** and 174.4° in **6d**).

Catalysis

As a preliminary comparison of the relative reactivity of complexes **6a–c** with that of those derived from neutral or other cationic phosphines, we initially evaluated their performance in the intramolecular hydroarylation of sulfide **7** into thiepine **8** following a *7-exo-dig* cyclisation.[24] The conversion versus time plot for the different precatalysts under otherwise identical conditions (2 mol% [Au], 2 mol% $AgSbF_6$, r.t., CD_2Cl_2) is shown in Figure 7. To put our results into perspective, neutral phosphole **9**, cationic phosphine **10**, and phosphite Au complexes **11**, were also prepared and used as precatalyst under otherwise identical reaction conditions (See the Supporting Information).

As expected, all cationic precatalysts tested performed better than **9**. In addition, comparison of the plots obtained with **6b** and **10** allows assessing the effect of the phosphole unit; this moiety makes **6b** slightly more reactive than **10** and, interestingly, it seems to confer longer life to the catalytic species. Phosphite complex **11** depicts intermediate performance between **6b** and **10**. The most promising results in terms of conversion were provided by **6c** containing the most strongly π-acceptor, cAAC-derived cationic moiety. We attribute the poor performance of **6a** when compared to **6b** to the higher steric demand imposed by the IMes moiety.

Finally, the catalytic performance of the Au complexes **6a–c** was additionally evaluated in the Au-catalysed cyclisation of *N*-(3-iodoprop-2-ynyl)-*N*-tosylanilines **12a–c** into the corresponding 1,2-dihydroquinolines. This particular transformation was chosen because two regioisomeric products are known to be produced; those derived from simple cyclisation **13a–c**, and compounds **14a–c**, which additionally involve a 1,2-iodo migration concomitant to the cycloisomerization. Moderate π-acceptor ligands attached to Au, as the phosphite in complex **11** have been reported to favor the first pathway

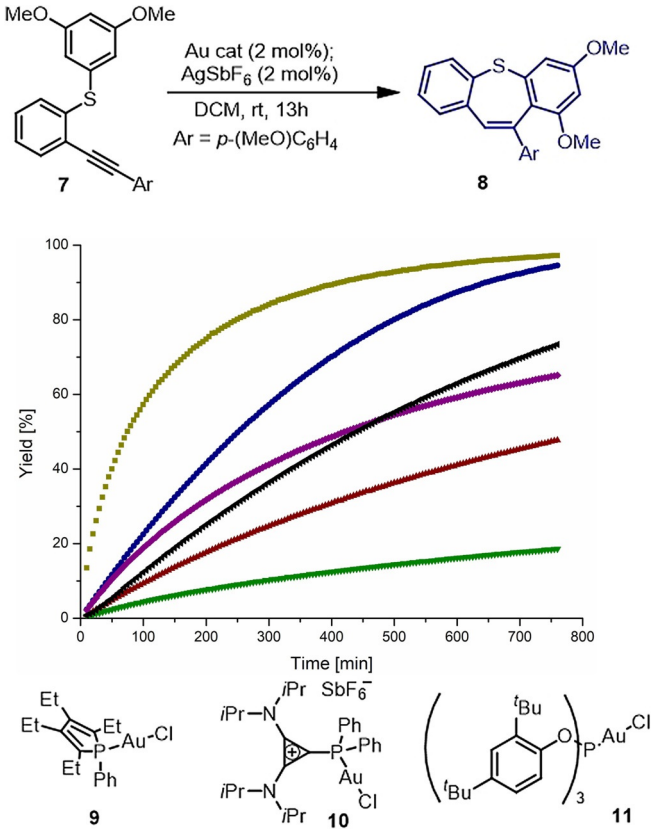

Figure 7. Ligand effect on the Au-catalyzed hydroarylation of diaryl sulfide **7** into thiepine **8.** Conditions: **7** (0.045 M in CD_2Cl_2), Au precatalysts (2 mol%), $AgSbF_6$ (2 mol%), r.t. Conversions determined by ^{1}H-NMR. Color code: **9** (▼); **6a** (▲); **11** (◀); **10** (■); **6b** (●); **6c** (■).

(Table 1, Entry 1); while strong σ-donating NHCs preferentially induce a 1,2-iodine shift prior to the cyclisation event (Table 1, Entry 2).[25] Hence, this transformation seems to be ideal to further tests the unique donor properties of ligands **2a–c.** Discrimination between competing reaction pathways and not only a kinetic effect is expected here.[26]

The product ratio obtained using precatalysts **6b** is comparable to those afforded by **10** and **11**, confirming the donor ability rank previously stablished. The selectivity towards **13a** improves when precatalyst **6a** is employed, and reaches a remarkable 97:3 ratio for cAAC-derived **6c** (Table 1, Entries 3–5). Identical tendency is observed for substituted substrates **12b** (R = Cl) and **12c** (R = C(O)Me) (Table 1, Entries 7–11). Especially remarkable is the effect of precatalyst **6c** in the cyclisation of **12b**. In this case the phosphole ligand is even able to invert the product distribution of the reaction if compared to **11** and **15** (entries 7–9). Compound **13b** is thus by far the major product of that reaction with a **13b**:**14b** ratio of 97:3.

Conclusion

An efficient method for the preparation of α-cationic phospholes differing on the nature of the cationic group is reported, together with the synthesis of their Au-complex derivatives. Our experiments suggest exceptional electrophilicity at the Au center that can be used to accelerate otherwise difficult transformations and importantly, to discriminate between competing reaction pathways. Given the easy handling of ligands **2a–d**, we suspect that a potentially large number of Au-catalyzed transformations might benefit from their use. Ongoing research in our group is focused in this direction. We also target the application of cationic phosphole ligands in processes catalyzed by metals other than Au.

Table 1: Effect of α-cationic phosphole ligands of different π-acceptor ability on the outcome of the Au-catalyzed cyclisation of tosylanylines **12a–c**.

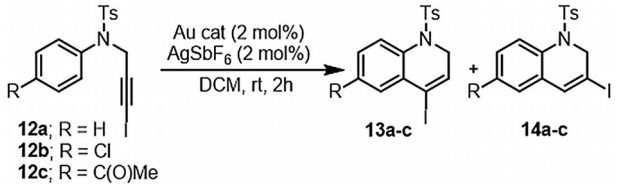

Entry	Substrate	Au cat.	Conv (%)[b]	**13:14** ratio[c]
1[a]	**12a**	**11**	(64)	58:42
2[a]	**12a**	**15**	(85)	7:93
3	**12a**	**6a**	>95	75:25
4	**12a**	**6b**	>95	56:44
5	**12a**	**6c**	>95 (80)	97:3
6	**12a**	**10**	>95	59:41
7[a]	**12b**	**11**	(79)	31:69
8[a]	**12b**	**15**	(80)	<1:99<
9	**12b**	**6c**	>95 (79)	97:3
10[a]	**12c**	**11**	67	78:22
11	**12c**	**6c**	>95(95)	99:1

[a] Results from ref. [24a]. [b] Conversions determined by ^{1}H NMR of the crude reaction mixtures; in parenthesis isolated yields; [c] Isomeric ratios determined by ^{1}H NMR.

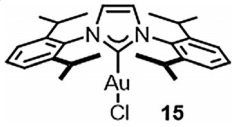

Acknowledgements

Financial support from the Deutsche Forschungsgemeinschaft (AL 1348/8-1, INST 186/1237-1 and INST 186/1324-1) and the European Research Council (ERC CoG 771295) is gratefully acknowledged. We thank K. Sprenger for the preparation of **7** and initial kinetic experiments and Prof. M. Bennati, Dr. I. Tkach and Dr. A. Meyer (MPI für Biophysikalische Chemie, Göttingen) for help with EPR analyses. Open access funding enabled and organized by Projekt DEAL.

Conflict of interest

The authors declare no conflict of interest.

Keywords: Au catalysis · cationic ligands · hydroarylation · ligand design · phospholes

[1] a) X. Zhao, S. T. Chaudhry, J. Mei, *Adv. Heter. Chem.* **2017**, *121*, 133 – 171; b) R. Réau, P. W. Dyer, *Phospholes. Comprehensive Heterocyclic Chemistry III*, Elsevier, Amsterdam, **2008**, pp. 1029 – 1147; c) D. B. Chesnut, L. D. Quin, *Heteroat. Chem.* **2007**, *18*, 754 – 758; d) L. D. Quin, *Phospholes. Comprehensive Heterocyclic Chemistry II*, Elsevier, Amsterdam, **1996**, pp. 757 – 856; e) F. Mathey, *Chem. Rev.* **1988**, *88*, 429 – 453.

[2] a) A. D. Becke, *J. Chem. Phys.* **1993**, *98*, 5648 – 5652; b) C. Lee, W. Yang, R. G. Paar, *Phys. Rev. B* **1988**, *37*, 785 – 789.

[3] The hyperconjugative interaction between the exocyclic P–R bond and the dienic fragment has been proposed to play a non-negligible role on the aromatic stabilization in phosphole rings.

[4] a) M. Hissler, C. Lescop, R. Réau, *Compt. Rend. Chim.* **2008**, *11*, 628 – 640; b) F. Mathey, J. Fischer, J. H. Nelson, *Complexing modes of the phosphole moiety. Transition Metal Complexes Structures and Spectra*, *Vol. 55*, Springer, Berlin, **1983**, pp. 153 – 201.

[5] a) C. Thoumazet, H. Grüztmacher, B. Deschamps, L. Ricard, P. le Floch, *Eur. J. Inorg. Chem.* **2006**, 3911 – 3922; b) J. J. MacDougall, J. H. Nelson, F. Mathey, J. J. Mayerle, *Inorg. Chem.* **1980**, *19*, 709 – 718.

[6] For a review about the use of phospholes as ancillary ligands in catalysis see: K. Fourmy, D. H. Nguyen, O. Dechy-Cabaret, M. Gouygou, *Catal. Sci. Technol.* **2015**, *5*, 4289 – 4323.

[7] a) L. D. M. Nicholls, M. Alcarazo, *Chem. Lett.* **2019**, *48*, 1 – 13; b) M. Alcarazo, *Acc. Chem. Res.* **2016**, *49*, 1797 – 1805; c) M. Alcarazo, *Chem. Eur. J.* **2014**, *20*, 7868 – 7877.

[8] a) L. Gu, L. M. Wolf, A. Zieliński, W. Thiel, M. Alcarazo, *J. Am. Chem. Soc.* **2017**, *139*, 4948 – 4953; b) G. Mehler, P. Linowski, J. Carreras, A. Zanardi, J. W. Dube, M. Alcarazo, *Chem. Eur. J.* **2016**, *22*, 15320 – 15327; c) E. Haldón, Á. Kozma, H. Tinnermann, L. Gu, R. Goddard, M. Alcarazo, *Dalton Trans.* **2016**, *45*, 1872 – 1876; d) Á. Kozma, J. Rust, M. Alcarazo, *Chem. Eur. J.* **2015**, *21*, 10829 – 10834; e) H. Tinnermann, C. Wille, M. Alcarazo, *Angew. Chem. Int. Ed.* **2014**, *53*, 8732 – 8736; *Angew. Chem.* **2014**, *126*, 8877 – 8881; f) J. Carreras, G. Gopakumar, L. Gu, A. Gimeno, P. Linowski, J. Petuškova, W. Thiel, M. Alcarazo, *J. Am. Chem. Soc.* **2013**, *135*, 18815 – 18823.

[9] a) H. Tinnermann, L. D. M. Nicholls, T. Johannsen, C. Wille, C. Golz, R. Goddard, M. Alcarazo, *ACS Catal.* **2018**, *8*, 10457 – 10463; b) J. W. Dube, Y. Zheng, W. Thiel, M. Alcarazo, *J. Am. Chem. Soc.* **2016**, *138*, 6869 – 6877.

[10] a) J. Zhang, M. Simon, C. Golz, M. Alcarazo, *Angew. Chem. Int. Ed.* **2020**, *59*, 5647 – 5650; *Angew. Chem.* **2020**, *132*, 5696 – 5699; b) T. Hartung, R. Machleid, M. Simon, C. Golz, M. Alcarazo, *Angew. Chem. Int. Ed.* **2020**, *59*, 5660 – 5664; *Angew. Chem.* **2020**, *132*, 5709 – 5713; c) L. D. M. Nicholls, M. Marx, T. Hartung, E. González-Fernández, C. Golz, M. Alcarazo, *ACS Catal.* **2018**, *8*, 6079 – 6085; d) E. González-Fernández, L. D. M. Nicholls, L. D. Schaaf, C. Farès, C. W. Lehmann, M. Alcarazo, *J. Am. Chem. Soc.* **2017**, *139*, 1428 – 1431.

[11] a) M. Westerhausen, C. Gückel, H. Piotrowski, P. Mayer, M. Warchhold, H. Nöth, *Z. Anorg. Allg. Chem.* **2001**, *627*, 1741 – 1750; b) P. Fagan, W. A. Nugent, J. C. Calabrese, *J. Am. Chem. Soc.* **1994**, *116*, 1880 – 1889.

[12] V. Lavallo, Y. Canac, B. Donnadieu, W. W. Schoeller, G. Bertrand, *Science* **2006**, *312*, 722 – 724.

[13] V. Lavallo, Y. Canac, C. Präsang, B. Donnadieu, G. Bertrand, *Angew. Chem. Int. Ed.* **2005**, *44*, 5705 – 5709; *Angew. Chem.* **2005**, *117*, 5851 – 5855.

[14] F. H. Allen, O. Kennard, D. G. Watson, L. Brammer, A. G. Orpen, R. Taylor, *J. Chem. Soc. Perkin Trans. 2* **1987**, S1 – S19.

[15] Deposition numbers 2006361, 2006362, 2006363, 2006364, 2006365, 2006366, 2006367, 2006368, 2006369 and 2006370 contain the supplementary crystallographic data for this paper. These data are provided free of charge by the joint Cambridge Crystallographic Data Centre and Fachinformationszentrum Karlsruhe Access Structures service.

[16] A. Kozma, T. Deden, J. Carreras, C. Wille, J. Petuškova, J. Rust, M. Alcarazo, *Chem. Eur. J.* **2014**, *20*, 2208 – 2214.

[17] $^{1}J_{P\text{-}Se}$ coupling constants are also used as reliable probe to assess the basicity of phosphanes. Unfortunately, only **2b** reacted with Se to afford the corresponding selenide, which is characterized by a $^{1}J_{P\text{-}Se} = 763$ Hz. This value suggests that **2b** is characterized by a donor capacity very similar to that of $[m\text{-}(CF_3)C_6H_4)]_3P$ ($^{1}J_{P\text{-}Se} = 766$ Hz). See: D. W. Allen, B. F. Taylor, *Dalton Trans.* **1982**, 51 – 54.

[18] H. Clavier, S. P. Nolan, *Chem. Commun.* **2010**, *46*, 841 – 861.

[19] L. Gu, Y. Zheng, E. Haldón, R. Goddard, E. Bill, W. Thiel, M. Alcarazo, *Angew. Chem. Int. Ed.* **2017**, *56*, 8790 – 8794; *Angew. Chem.* **2017**, *129*, 8916 – 8920.

[20] See ref. 2 and: a) S. Grimme, J. Antony, S. Ehrlich, H. Krieg, *J. Chem. Phys.* **2010**, *132*, 154104; b) F. Weigend, *Phys. Chem. Chem. Phys.* **2006**, *8*, 1057 – 1065.

[21] K. Fourmy, S. Mallet-Ladeira, O. Dechy-Cabaret, M. Gouygou, *Organometallics* **2013**, *32*, 1571 – 1574.

[22] a) K. Fourmy, M. Gouygou, O. Dechy-Cabaret, F. Benoit-Vical, *C. R. Chim.* **2017**, *20*, 333 – 338; b) H.-C. Su, O. Fadel, C.-J. Yang, T.-Y. Cho, C. Fave, M. Hissler, C.-C. Wu, R. Réau, *J. Am. Chem. Soc.* **2006**, *128*, 983 – 995; c) S. Attar, W. H. Bearden, N. W. Alcock, E. C. Alyea, J. H. Nelson, *Inorg. Chem.* **1990**, *29*, 425 – 433.

[23] A. Bondi, *J. Phys. Chem.* **1964**, *68*, 441 – 451.

[24] K. Sprenger, C. Golz, M. Alcarazo, *Eur. J. Org. Chem.* **2020**, DOI: 10.1002/ejoc.202001072.

[25] a) P. Morán-Poladura, S. Suárez-Pantiga, M. Piedrafita, E. Rubio, J. M. González, *J. Organomet. Chem.* **2011**, *696*, 12 – 15; b) V. Mamane, P. Hannen, A. Fürstner, *Chem. Eur. J.* **2004**, *10*, 4556 – 45575.

[26] The influence of phosphole ligands on the regiochemical outcome of Pt-catalysed cycloisomerizations has been previously reported: K. Fourmy, S. Mallet-Ladeira, O. Dechy-Cabaret, M. Gouygou, *Dalton Trans.* **2014**, *43*, 6728 – 6734.

Manuscript received: July 6, 2020
Revised manuscript received: August 23, 2020
Accepted manuscript online: August 27, 2020
Version of record online: October 8, 2020

